Multifunctional Electronic Textiles using Silver Nanowire Composites

Shanshan Yao,[†] Ji Yang,[‡] Felipe R. Poblete,[†] Xiaogang Hu,[§] Yong Zhu[*,†,§]*

[†]Department of Mechanical and Aerospace Engineering, North Carolina State University, Raleigh, North Carolina 27695, USA

[§] Joint Department of Biomedical Engineering at University of North Carolina-Chapel Hill and NC State University, Chapel Hill, North Carolina 27599, USA

[‡]MOE Key Laboratory for Intelligent Networks and Network Security, Xi'an Jiaotong University, Xi'an, Shaanxi, 710049, China

E-mail: yong_zhu@ncsu.edu

KEYWORDS: Nanomaterials, silver nanowires, electronic textiles, health monitoring, activity tracking, thermotherapy

ABSTRACT

Textiles represent an appealing platform for continuous wearable applications due to the exceptional combination of compliance, water vapor permeability, and comfortableness for long-term wear. We present mechanically and electrically robust integration of nanocomposites with textiles by laser scribing and heat press lamination. The simple and scalable integration technique enables multifunctional E-textiles without compromising the stretchability, wearability and washability of textiles. The textile-integrated patterns exhibit small linewidth (135 μm), low sheet resistance (0.2 Ω/sq), low Young's modulus, good washability, and good electromechanical performance up to 50% strain, which is desirable for wearable and user-friendly electronic textiles. To demonstrate the potential utility, we developed an integrated textile patch comprising four dry electrophysiological electrodes, a capacitive strain sensor, and a wireless heater for electrophysiological sensing, motion tracking, and thermotherapy, respectively. Beyond the applications demonstrated in this paper, the materials and methods presented here pave the way for various other wearable applications in healthcare, activity tracking, rehabilitation, and human-machine interactions.

INTRODUCTION

Wearable electronics that can conform to curvilinear and complex skin surface to continuously monitor an individual's activities offer new opportunities in the tracking of wellness, treatment of illness, and interactions with smart devices.[1, 2] Numerous wearable devices have been developed, including a variety of sensors, displays, energy harvesting and storage devices, and drug delivery systems.[3-5] Advances in the compliance and performance of wearable devices greatly promote the applications in continuous health monitoring, activity tracking, electronic skin and human-machine interactions. Compared to those with a single function, integrated multifunctional wearable devices allow for a comprehensive tracking of physiological parameters,[6, 7] multimodal electronic skin,[8, 9] interactive human machine interfaces,[10, 11] and on-chip therapeutic treatments[12] on a minimized platform. Significant progress has been made towards the realization of multifunctional wearable devices on elastomer substrates. Representative examples include epidermal electronics,[13] multiplexed sweat sensing system,[6] wearable diabetes monitoring and therapy system,[12] and gas permeable stretchable on-skin electronics.[14, 15] Being soft, lightweight, water vapor permeable, and comfortable, textiles provide an ideal platform for wearable devices that can be worn on a daily basis for long term. However, multifunctional wearable devices built on textile substrates are relatively unexplored.

Electronic textiles (E-textiles) have been realized using a variety of fabrication methods. They can be constructed by directly knitting, weaving, embroidering conductive fibers, or by coating, printing or laminating conductive materials onto the fibers or fabrics.[16-21] However, these technologies face challenges such as low conductivity,[22, 23] limited patterning resolution,[22, 24-27] poor electromechanical stability,[25, 27] increased elastic modulus of the textiles,[24, 28] and complex fabrication process[28, 29] (Table 1). In spite of noteworthy advances, E-textiles are currently limited

by the lack of robust fabrication techniques to integrate multifunctionality onto textiles in a simple, high-resolution, and versatile way without sacrificing the comfortableness and washability of textiles.

In this study, we address these challenges by employing soft electronic materials, deformable structures, and efficient processes to enable multifunctional E-textiles without losing the wearability, washability, and comfortableness of textiles.[30] Silver nanowire (AgNW) composites are integrated with textiles through a laser scribing patterning and a heat press lamination process. This is the first AgNW laminated E-textiles with well-controlled resolution, to the best of our knowledge. During the laser scribing process, arbitrary patterns with high resolution can be generated without the need of masks or stencils. Heat press offers a facile way to laminate the patterned AgNW nanocomposites with strong bonding onto textiles and well-maintained electrical properties. Our integration process results in highly conductive, stretchable, compliant and washable patterns on textiles, which are the building blocks for textile-based smart devices. Based on the textile laminated patterns, we further demonstrated an integrated patch that incorporates dry electrodes for electrophysiological sensing, a capacitive strain for motion sensing, and a wireless heater for thermotherapy.

RESULTS AND DISCUSSION

Figure 1a depicts the fabrication process of the E-textiles. To start, AgNW solution was uniformly coated onto a glass substrate with a Meyer rod. After evaporating the solvent, AgNWs were randomly distributed to form the percolation network (Figure S1a). Thermoplastic polyurethane (TPU) solution was spin-coated on top of the AgNW networks followed by evaporating the solvent and solidifying the TPU. AgNWs were embedded just below the surface of TPU. The majority of

AgNWs were embedded in the TPU with a small density of AgNWs exposed on the surface (Figure S1b and Figure 1c inset). The selection of TPU to embed the AgNWs has several advantages: 1) TPU solution can blend well into the AgNW percolation networks due to its good wettability of AgNWs and the resulting AgNW/TPU nanocomposites maintain excellent electrical conductivity (Figure 1b); 2) TPU is a stretchable, hot-melt adhesive that can form reliable bonding to textiles. To form the desired patterns, the AgNW/TPU nanocomposites were subjected to laser scribing according to a 2D CAD drawing (Figures S2a and S2b). During laser scribing, TPU and AgNWs under the scribing path were melted and accumulated on the remaining pattern (Figures S2c and S2d). As a result of the melting effect, the linewidth in the final pattern would be 75 ± 10 μm smaller than that was defined in the CAD drawing. The linewidth in the final pattern will be used for the rest of the study. The AgNW/TPU patterns were then heat-pressed at 140 ºC to transfer from the glass substrate onto a stretchable fabric. The final textile-integrated AgNW/TPU patterns are highly conductive, compliant, stretchable and washable, ideal for E-textiles applications.

Figure 1b displays the sheet resistances of the AgNWs coated on the glass substrate, AgNWs/TPU nanocomposites on the glass substrate, and AgNW/TPU laminated on textiles for different AgNW densities, respectively. It can be found that the sheet resistance increases after introduction of insulating TPU and slightly decreases after heat press. Mechanical compression and thermal annealing, as reported in the previous work,[31, 32] reduce the contact resistance between AgNWs, leading to the enhanced conductivity after heat press. Figure 1c shows the patterned AgNW/TPU nanocomposites on textiles with different linewidths. For linewidths ranging from 135 μm to 500 μm, the sheet resistance was measured to be around 0.2 Ω/sq and the conductivity to be around 5030 S/cm (Figure 1d). It is challenging to create well-controlled patterns with linewidth below 135 μm due to the defects caused by melting during the laser scribing process.

To test the electromechanical stability of the laminated AgNW/TPU on textiles, the samples with different patterns were mounted onto a motorized tensile stage to apply the strain. As shown in Figure 2a, for a straight-line pattern, the resistance increased dramatically during the first stretching/releasing cycle with a tensile strain of 50%. The resistance did not revert to the original value upon releasing the strain, mainly due to the irreversible sliding of the AgNWs in the polymer matrix.[33] Following the approach of prestrain-release-buckling,[30] a more stable resistance under strain was achieved. As an example, the textile substrate was prestrained by 30% before heat pressing the AgNW/TPU patterns onto the textile. After releasing the prestrain, a buckling structure was generated in the AgNW/TPU nanocomposites (Figure 2a inset). During the following stretching, the buckling structure accommodated most of the strain and relieved the strain experienced by the AgNW/TPU nanocomposites. As a result, the resistance change under strain was significantly decreased (Figure 2b). Then two other patterns used in the integrated textile patch, i.e. Greek cross fractal patterns for dry electrodes and coil patterns for wireless heater, were transferred onto the prestrained textiles and tested. A Greek cross fractal pattern was chosen for the electrophysiological electrodes, mainly due to its good stretchability and a high level of connectivity (and thus minimized resistance). This design supports robustness in mechanical and electrical properties of the pattern.[34] At the 11st cycle of stretching with 30% strain, 6%, 4% and 2% increase in the resistance was observed for the straight line, fractal and coil patterns, respectively, indicating good electromechanical stability.

Stress-strain curves of the original textiles and textiles with AgNW/TPU patterns were measured to assess the mechanical properties of the integrated textiles (Figure 2c). Owing to the excellent compliance of the nanocomposites and the introduction of stretchable structures (e.g. wavy structure and fractal patterns), the Young's modulus of the AgNW/TPU laminated E-textile was

only 0.38 MPa, comparable to modulus of the epidermis of human skin.[13] The result illustrates the sufficient softness of the E-textile for skin wear. Moreover, the washability of the textile integrated AgNW/TPU fractal patterns were tested according to the standard ISO 6330:2000. The samples in a laundry bag were placed into the washing machine together with ballast to reach 2 kg standard load. The samples were drip dry at room temperature after each washing process. Figure 2d summarizes the resistance change as a function of the washing cycle. The resistance change increased around 10% after 100 washing cycles, which is considered to be due to the combined effects of mechanical distortion, thermal stress and moisture.[35, 36] The increase in resistance during washing is lower than that for screen printed Ag/AgCl inks on TPU,[24] Cu-PET yarns,[37] sewn conductive threads,[38] PEDOT:PSS coated knitted fabrics,[39] and comparable to that of liquid metal enabled elastomeric microfibers.[36] The encapsulation by TPU is conducive to the better resistance to washing process owing to the reduced delamination of AgNWs. To further test the performance after long-term scrubbing with skin, the E-textile was attached onto the forearm and scrubbed against the skin by holding the two ends of the E-textile and sliding it on the skin with 20 mm offset. Around 4% increase in resistance was observed after scrubbing on skin for 1000 cycles (Figure S4).

The water vapor transmission of the original textile and the textile with laminated AgNW/TPU patterns was tested to assess the moisture permeability and the result was given in Figure S5. The water vapor transmission was 114.2 and 108.3 g/m^2 h before and after laminating AgNW/TPU patters, indicating a small decrease of 5.2%. Since AgNWs were introduced into the E-textile, a piece of E-textile with AgNW density of 0.48 mg/cm^2 was worn the forearm and only took off during the shower to evaluate the skin biocompatibility. No obvious changes in skin under the E-textile, such as itching or erythema, were observed during and after 1 week of wearing (Figure

S6). Moreover, it was previously demonstrated that Ag nanoparticles and Ag nanowires composites exhibited evident antimicrobial efficiency due to the release of silver ions.[40] More detailed studies on the cytotoxicity effect, skin biocompatibility, and antibacterial effect of AgNW/TPU composites are underway.

To illustrate the potential applications of the E-textiles, three devices were integrated into a textile patch (Figure 3), demonstrating sports applications. The patch is stretchable, foldable and twistable (Figure 3c), as expected during sports activities. Three dry electrodes with Greek cross fractal patterns were fabricated for electrophysiological applications. These electrodes can be used to record both heart activities (electrocardiography, ECG) and muscle activities (electromyography, EMG), which are of great interest for tracking sports performance. Heart rate can be readily derived from the R–R interval of the ECG signal. Beyond heart rate, ECG recording represents one of the most commonly used tools to diagnose and manage cardiovascular diseases, the leading cause of death. EMG sensing plays an important role in evaluating the health of muscle tissues and nerves, and in diagnosing neuromuscular disorders and motor neuron dysfunctions.[41] It is worth noting that the electrodes demonstrated here are dry, eliminating the conductive gel that is commonly used in commercial disposable electrodes. The dry electrodes address the major challenges faced by pre-gelled electrodes for long-term applications – signal quality degradation caused by dehydration of the gel with time, potential skin irritation evoked by the gel, and the inconvenience associated with repeatedly reapplication of new gel.[41]

The electrode-skin impedance of the commercial gel electrodes and the fabricated dry textile electrodes were measured by placing two electrodes on the forearm with the electrodes 30 mm apart (center-to-center). Without the gel, the dry textile electrodes exhibited only slightly higher electrode-skin impedance than commercial gel electrodes, owing to the excellent compliance and

very high conductivity (Figure S7). Upon 50% strain, the electrode-skin impedance of the dry electrodes marginally increased.

ECG signals were captured using the right electrode as the recording and the back electrode as the reference (Figure 3). The recording electrode was in contact with the left forearm and the reference electrode was touched by the right index finger (Figure 4a) to form a configuration similar to a Lead I ECG. The gathered signals from the commercial gel electrodes and dry textile electrodes were comparable (Figure 4b), and no apparent signal degradation was observed for stretched dry textile electrodes at 50% strain and for dry textile electrodes after 100 cycles of washing (Figure S8). The P wave, QRS complex, and T wave can all be clearly identified on the curves. For the surface EMG measurement, the recording (right), reference (left) and ground (middle) electrodes were placed on the forearm, parallel to the muscle fiber direction. EMG signals corresponding to the muscle contraction during the fist clenching can be clearly detected (Figure 4c). Comparable EMG signals were obtained from the commercial gel electrodes and from the unstretched, stretched, and washed dry textile electrodes, respectively (Figure 4d and Figure S9). These results indicate that AgNW-based textile electrodes, in a dry and wearable form, can be employed to measure high quality ECG and EMG signals.

The laminated AgNW/TPU nanocomposites can also be combined with other soft materials to realize textile-based wearable applications. As an example, a capacitive strain sensor using AgNW/TPU and AgNW/Ecoflex nanocomposites was incorporated into the E-textile patch to track the body movements. Here a capacitive sensor design modified from our previous work was employed.[42, 43] As shown in the schematics in Figure 5a, the top electrode of the stretchable capacitor was made by embedding AgNWs just below the surface of a highly compliant elastomer (Smooth-on Ecoflex 0030).[43] For the bottom electrode, AgNWs were firstly embedded in TPU for

selected areas. A layer of liquid Ecoflex was then coated onto the remaining AgNW areas while exposing enough TPU area to provide a strong bonding to the textile. The structure ensures a sufficiently low Young's modulus of the sensor so as not to disrupt the natural body movements. The top and bottom electrodes were then sandwiched by a thin layer of Ecoflex as the dielectric with the AgNW side face to face. The elongation of the stretchable capacitor leads to an increase in the capacitance,[42, 44] as shown in the calibration curves in Figure 5b. The gauge factor of the capacitive strain sensor, defined as the change in the capacitance (C) divided by the applied tensile strain (ε), $GF = (\Delta C / C_0) / \varepsilon$, was calculated to be 0.96 over a strain range up to 50%. The gauge factor is close to the theoretical limit of 1 and among the highest reported value for the stretchable capacitive strain sensors.[43, 44] The correlation between the capacitance change and the strain is linear and reversible. The strain sensing range is sufficient for the strain level associated with typical human motions.[42, 43, 45, 46] The fabricated strain senor was subjected to cyclic loading and unloading of 50% strain to obtain the stability of the strain sensor. As can be seen from Figure S10, the change in gauge factor of the strain sensor was within 0.02 during 500 cycles of loading and unloading. The good stability is consistent with the reported capacitive strain sensors based on elastomer substrates.[43, 47]

The strain sensor was mounted onto the elbow (Figure 5c) to monitor the elbow bending at different bending speeds (Figure 5d). We found that the measured strain from the strain sensor is linearly proportional to the bending angle of the elbow (Figure 5e). This can be explained by assuming the elbow joint as a hinge-type joint, as shown schematically in Figure 5f.[48] The change in skin length along the bending direction can be approximated as $\Delta l = r\theta$, where r is the radius of the joint and θ is the bending angle. The strain experienced by the skin during elbow bending is thus $\varepsilon = \Delta l / l_0 = r\theta / l_0$, where l_0 is the initial length of the skin. Therefore, the strain measured by

the strain sensor is expected to be proportional to the bending angle. By converting the strain to bending angle and taking the derivative, the angular velocity associated with the elbow bending can be calculated. Bending angle and angular velocity are more straightforward parameters to be used by athletes and trainers. In this demonstration, we showed that from the wearable textile integrated strain sensors, important motion parameters including bending angle, strain, and angular velocity can all be obtained in real time. Such quantitative data provide valuable information to quantitatively evaluate athletic performances, improve postures, prevent injuries, and facilitate rehabilitation.

Thermotherapy or heat therapy is widely used during rehabilitation to relieve pain and facilitate healing of sport injuries. It can take various forms, including heat pack, hot water bottle, hot shower, whirlpool bath, steam bath, sauna, and others. Heat can alleviate pain, increase blood flow, relieve muscle spasms, decrease joint stiffness, and reduce inflammation.[49, 50] Here we integrate a wireless heater with the textiles to enable thermotherapy in a wireless and wearable manner. The wireless heating mechanism is similar to wireless charging.[51] Both of them rely on inductive wireless energy transfer. Wireless charging uses a receiver inductor with an extreme low resistance to minimize the energy loss in the inductor and thus the transmitted energy can be used to charge a device. Wireless heating includes a resistive receiver inductor that converts the transmitted electrical energy into heat. As schematically illustrated in Figure 6a, during wireless heating, alternating current in the transmitter coil (housed in the charger) generates an oscillating magnetic field, which induces a current in the receiver coil (the heater coil). Due to the resistive nature of the heater coil, the current flowing within the coil produces heat through joule heating.

Our wireless heater can be powered by any commercial Qi standard wireless charger. The heater is designed to achieve the recommended temperature range for thermotherapy (between 40 ^{o}C to

45 ºC).[52, 53] Figure 6b shows the temperature distribution of the heater, taken using an infrared (IR) camera, after being powered for 1 minute. Since silver has a very low emissivity, the AgNW/TPU heater appears "cold" in the thermal image.[54, 55] The true temperature is better reflected in the textile. For this reason, the IR images from the backside of the heater were taken for the rest of the study. Figure 6b-6e compare the temporal profile and the temperature distribution of the heater without strain and with 30% uniaxial strain, respectively. Under stretching, the temperature is slightly higher than that of the unstrained state, which can be attributed to the enlarged area of the heater coil (receiver coil) during stretching and the resulting higher transmitted energy in the heater.[51] The heating process took ~30 s to reach the desired temperature for both unstretched and stretched heater (Figure 6e). The heating time is similar to that of the wireless heater based on copper-clad polyimide film[56] and much shorter than that of the wireless heater based on patterned zinc foil.[51] The results illustrated the potential utility of the textile integrated wearable wireless heater for therapeutic heating.

The simple and direct patterning method of AgNW based textiles we reported here can achieve high resolution and high throughput. Several direct writing techniques have been developed for AgNWs, including gravure printing,[57] screen printing,[58] electrohydrodynamic (EHD) printing,[59, 60] and inkjet printing.[61] High resolution of 50 μm was achieved on plastic, paper, or elastomer substrates.[57-60] These printing techniques, however, cannot be simply extended to textile substrates with comparable resolution due to large surface roughness and different surface properties from plastics/elastomers. More specifically, inkjet printing requires the AgNWs to be shortened to avoid nozzle clogging during printing, which however sacrifices the advantage of high-aspect-ratio nanowires.[61] Screen printing,[58] EHD printing,[59, 60] and gravure printing[57] require the introduction of additives to adjust the viscosity of the ink. An extra water rinsing step in the post-processing is

needed to remove the additives, which may cause delamination of AgNWs from textiles especially when scrubbing against skin and/or during washing process.

CONCLUSION

In summary, we report facile textile integration of AgNW/TPU nanocomposites for multifunctional E-textiles based on laser direct scribing and heat press lamination. We demonstrated the first AgNW laminated E-textiles with well-controlled resolution and robust stability during washing and stretching. A minimal linewidth of 135 μm and sheet resistance of 0.2 Ω/sq were achieved for the laminated AgNW/TPU patterns on textiles. The increase in resistance was found to be less than 6% under tensile strain up to 30%. The integrated textiles exhibited comparable mechanical properties to the original textiles, and stable electrical performance after many cycles of washing. Based on the textile laminated patterns, we further demonstrated highly integrated multifunctional E-textiles with comparable resolution to those based on polymer substrates. The integrated patch consisting of four dry electrophysiological electrodes, a capacitive strain sensor, and a wireless heater was designed and fabricated. The results demonstrated the capability of ECG/EMG sensing, body motion sensing, and thermotherapy in a single wearable textile patch, which are all of important relevance to sports applications. Features like excellent electrical performance, wearability, and washability promise the wide applications of the multifunctional E-textiles. For example, the collected physiological and body activity parameters can provide valuable insights into the well-being and fitness of human body. The E-textiles offer a convenient tool to quantify body motions and provide feedback for prosthetics and robotics. In addition to the functions demonstrated in this work, other wearable functions such as touch,[62] skin impedance,[63] and antenna[64] can be readily integrated into textiles using this technique.

METHODS

Textile integration of AgNW based nanocomposites. The synthesis of AgNWs followed a modified polyol reduction method.[57] The diameter of the AgNWs was 89.3 ± 17.5 nm and the length was 23.4 ± 5.7 μm, calculated from 100 NWs. The synthesized nanowires were dispersed into ethanol with concentration of 5 mg/ml for the subsequent coating process. AgNW solution was coated onto the glass substrate using Meyer rod coating (RD Specialties) followed by drying at 50 ºC on a hotplate. More cycles of coating and drying were performed to achieve the desired AgNW density. The mass of the AgNWs can be calculated from the concentration and volume of the AgNW ink used for the coating. The AgNW density can be determined by dividing the mass by the coating area. The TPU (Perfectex plus LLC) was dispersed in dimethylformamide (DMF) into concentration of 0.25 g/ml. The TPU/DMF solution was then spin coated over the AgNW networks at 250 rpm for 30 s. The solvent was evaporated at 120 ºC on a hotplate for 1 h to solidify the TPU and embed the AgNWs into TPU. Next, the AgNW/TPU nanocomposites were patterned into desired shapes using a laser cutter (Universal VLS 6.60, Epilog Laser) with a cutting speed of 100% and power of 10%. The patterns were subsequently pressed onto textiles at a temperature of 140 ºC for 30 s using a digital heat press machine (Fancierstudio). After removing the glass substrate, AgNW/TPU patterns were transferred onto the textiles. For wireless heater, the two ends of the heater coil on the front side and the connector on the back side need to be connected (Figure 6a). Conductive Cu wires were penetrated through the textile to serve as through-textile interconnects. The two ends of Cu wires were electrically connected with the AgNW/TPU patterns on both sides by drop-casting a small droplet of Ag stretchable printing ink (Engineered Materials Systems, CI-1036) followed by thermal treatment at 100 ºC for 5 min to remove the solvent in the ink and secure the bonding between Cu wires and AgNW/TPU patterns.

Characterization of AgNW/TPU laminated textiles. Stress-strain curves of the textile with and without AgNW/TPU patterns were obtained using a mechanical tester (DTS Company) at a loading speed of 0.05 mm s^{-1}. Sheet resistance (R_s) of the fabricated E-textiles was measured using the four-point probe method with a digital multimeter (34401A, Agilent) and corrected with geometric factors.[65] The conductivity (σ) was calculated by $\sigma = 1/R_s t$ (t is the averaged thickness). For electromechanical testing, the textiles were mounted onto a lab-made tensile stage and subjected to cycles of stretching and releasing. Meanwhile, the resistance of the AgNW/TPU patterns on textiles under strain was measured by a digital multimeter (34401A, Agilent). The washability of the fabricated electronic textiles was tested according to the international standard ISO 6330:2000. The samples were placed in a laundry bag with 2 kg of ballast to reach 2 kg standard load. The "delicate" option was chosen for the washing process. Between each washing cycle, the samples were drip dry at room temperature. The resistance of the AgNW/TPU pattern on textiles was measured after every 5 cycles. The water vapor transmission was tested according to ASTM standard E96 water method. Briefly, the sample was placed on a water dish with 90 mm in diameter. The weight of the tested dish was recorded at a temperature of 35 ºC and relative humidity of 65% over 48 hours. Water vapor transmission was calculated from the weight loss before and after the test. ECG and EMG measurements were performed using an amplifier (PowerLab 4/26, ADInstruments) with a sampling rate of 1 kHz per channel. The electrode-skin impedance was measured using a potentiostat (Reference 600, Gamry Instruments). The capacitance of the fabricated capacitive strain sensors was measured using a capacitance-to-digital converter evaluation board (AD7152, Analog Devices) with a sampling frequency of 50 Hz. To measure the gauge factor, the strain sensor was stretched on a tensile stage, with the capacitance measured at the same time. To test the heating performance, the wireless heater was powered by a

commercial Qi wireless charger (Armike Inc.). The temperature of the heater was obtained in real time with an infrared camera (A655SC FLIR) placed right over the heater.

Table 1. Summary of the performances of representative E-Textiles reported.

Materials	**Manufacturing techniques**	**Resolution**	**Conductivity**	**Young's modulus** (compared to original textiles)	**Stretchability**	**Washability**
CNT/PU[22]	Screen printing	1.5 cm	0.2 kΩ/sq	–	–	<10% increase in resistance after being immersed in water for 20 hours
CNT@Silk[23]	Electrospinning, sewing	–	310 S/cm	–	2% increase in resistance at 6.5% strain	–
Ag/AgCl/TPU[24]	Screen printing	1 mm	5000 S/cm	37 times increase	29% increase in resistance (meandering shaped) at 40% strain	62% increase in resistance after 100 cycles
Ag flake[25]	Screen printing	0.5 mm	0.06 Ω/sq, ~1333 S/cm (considering thickness of 125 μm)	Slightly increase	~300% increase in resistance at 50% strain, 70 times at 450% strain	No electric conduction after 50 cycles.
Plated Cu[26]	Electroless plating	2.5 mm	0.5 Ω/sq	–	–	–
Ag flake/TPU[27]	Screen printing	1 mm	4.31×10^4 S/cm	–	20 times increase in resistance at 50% strain	–
Cu/PDMS[28]	Lithography, liquid injection moulding, screen printing	–	–	> 3 times increase	–	No damage after 50 cycles
PI/Cu/PI/UL-Sil[29]	Photolithography	60 μm	–	Slightly increase	Almost no change up to 200% strain	Functional after 20 cycles
AgNW/TPU (this work)	Laser scribing, heat press	135 μm	0.2 Ω/sq, 5030 S/cm	~13% increase	21% increase in resistance (fractal pattern) at 50% strain	10% increase in resistance after 100 cycles

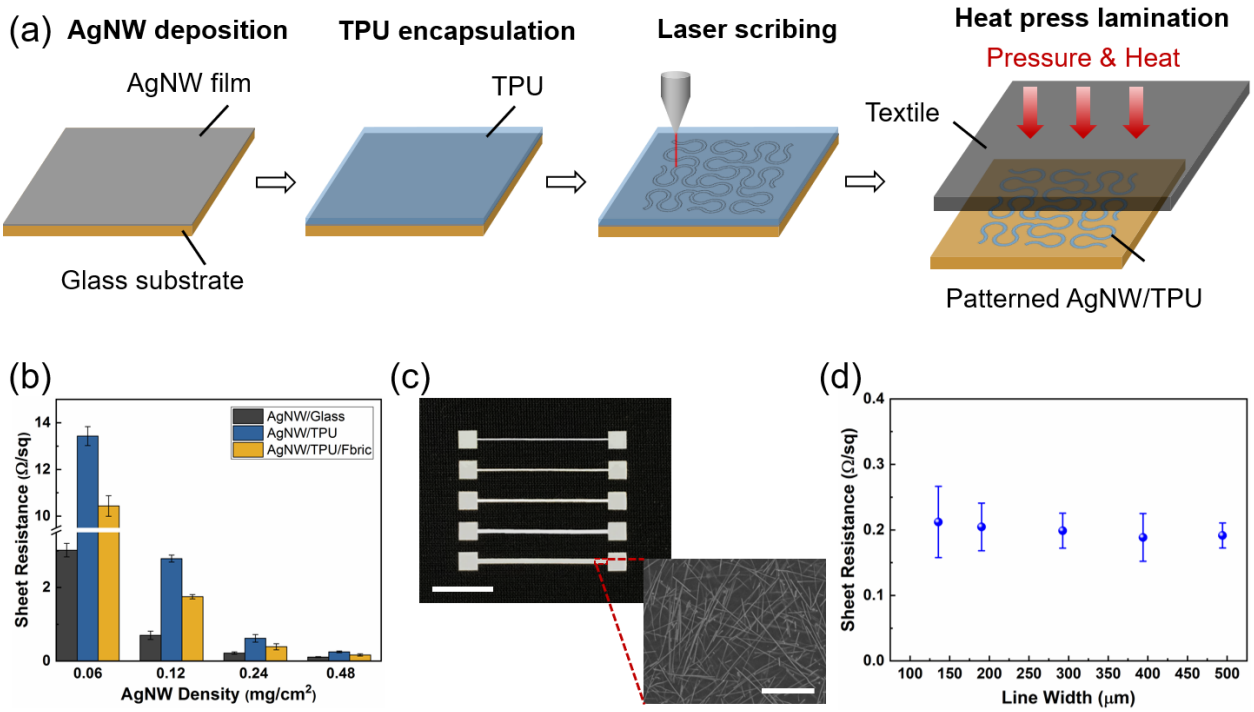

Figure 1. (a) Fabrication process for the textile integration. (b) Comparison of sheet resistance for AgNWs on glass substrate, AgNW/TPU nanocomposites, and AgNW/TPU laminated on textiles respectively at different AgNW density. Linewidth: 200 μm. (c) Laminated AgNW/TPU patterns with different linewidth with AgNW density of 0.48 mg/cm^2 (scale bar: 5 mm). The inset shows the top view SEM image of the AgNW/TPU pattern (scale bar: 5 μm). (d) Sheet resistance of laminated AgNW/TPU on textiles with different linewidths.

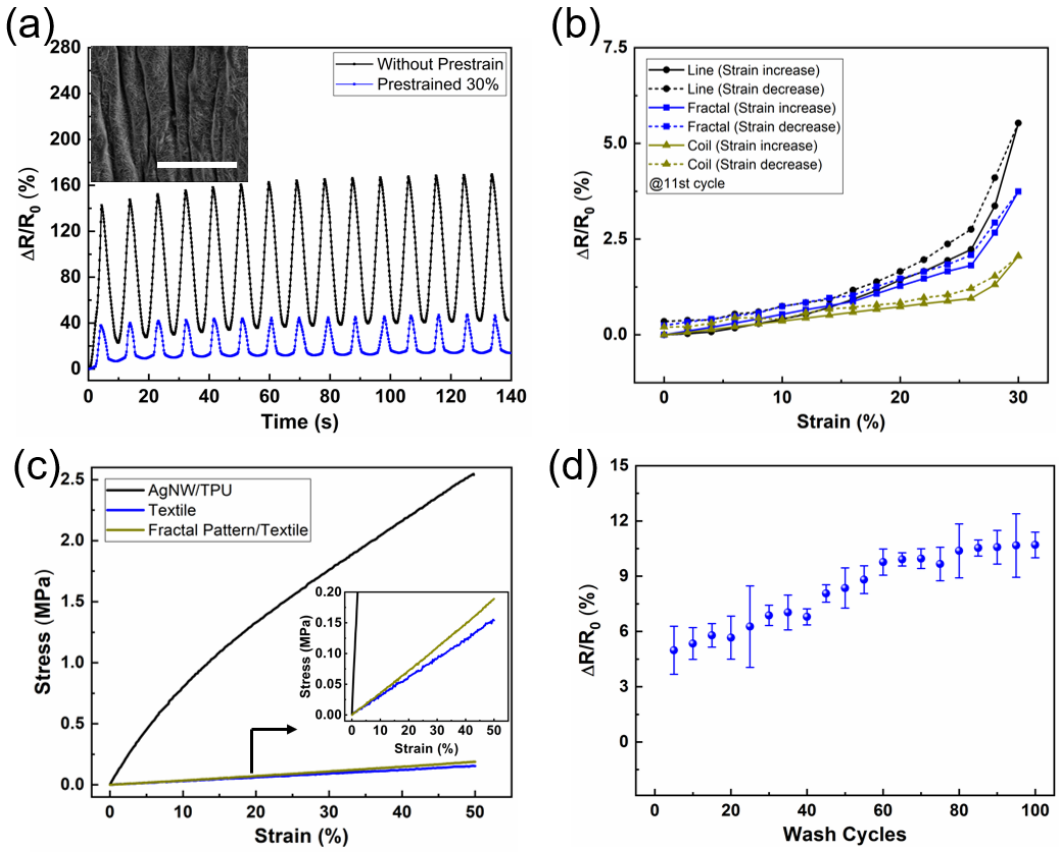

Figure 2. (a) Resistance change of AgNW/TPU patterns laminated on original and prestrained textiles under cyclic strain up to 50%. The inset shows the SEM image of the buckling structures in AgNW/TPU after releasing the prestrain. Scale bar, 50 μm. (b) Resistance change of AgNW/TPU patterns laminated on pretrained (30%) textiles as a function of strain (up to 30%) for different patterns. The results for 50% strain are given in Figure S3. (c) Stress-strain curves for the textile, AgNW/TPU composites, and fractal patterns laminated on textiles. The inset shows the enlarged view of the stress-strain curve. (d) Relative resistance changes of AgNW/TPU patterns laminated on textiles as a function of washing cycles.

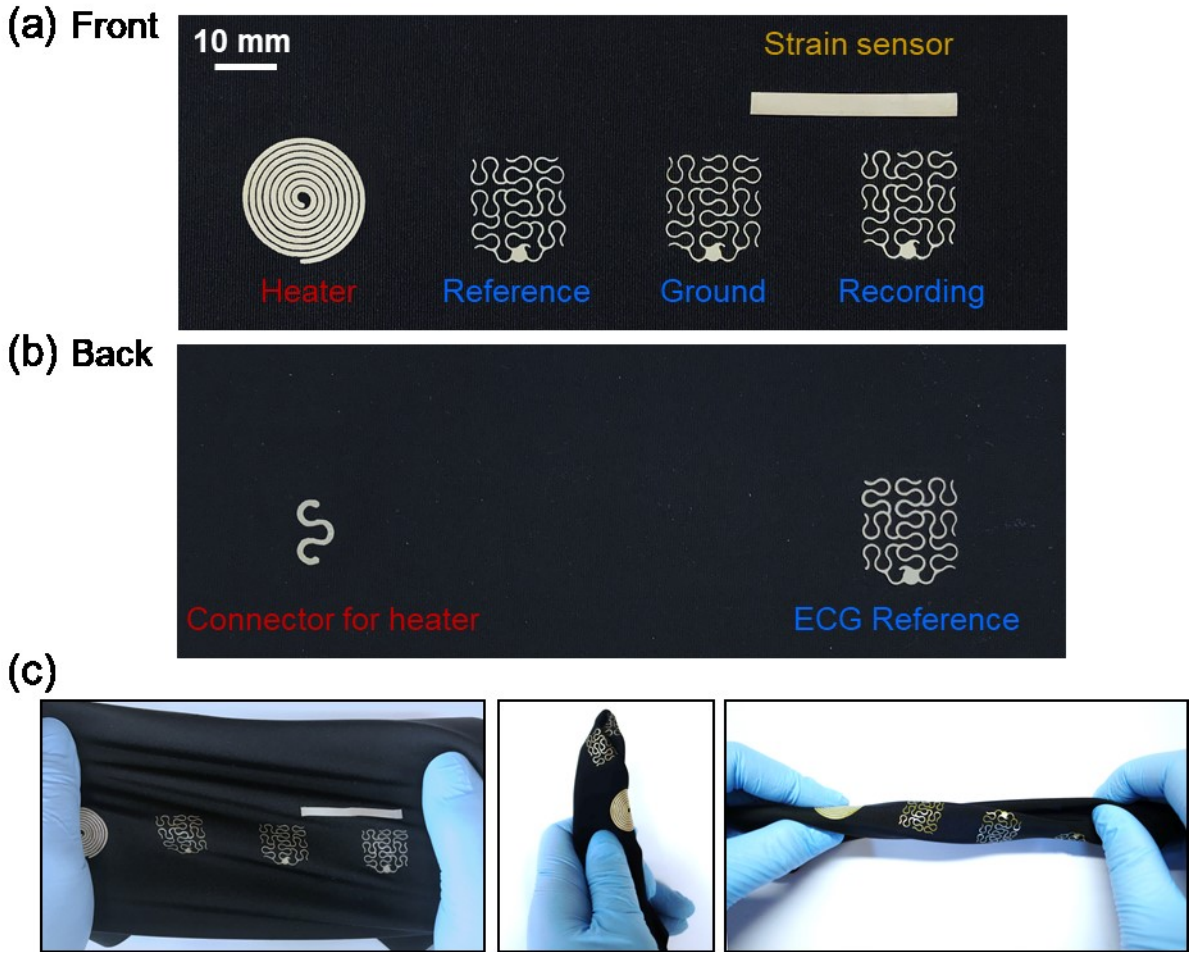

Figure 3. Integrated textile patch consisting of four dry electrodes (three are in the front), a capacitive strain sensor and a wireless heater for sports applications. (a) A picture of the front side of the patch. (b) A picture of the back side of the patch. Note the pictures were taken before interconnecting the coil heater on the front side and the connector on the back side. (c) The patch being stretched, folded and twisted.

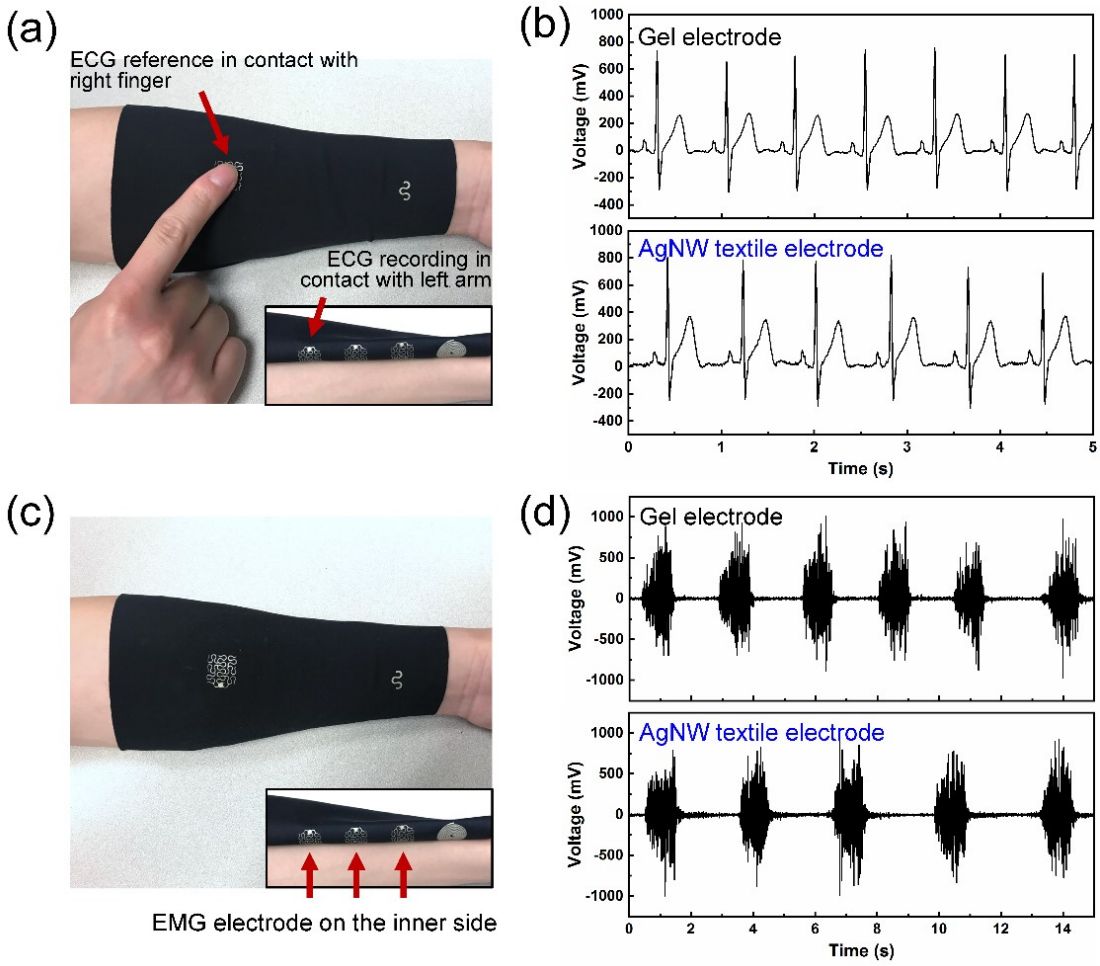

Figure 4. Performance of dry AgNW based textile electrodes for ECG and EMG sensing. (a) Pictures showing the configuration of ECG measurements. (b) Comparison of ECG signals between commercial gel electrodes and dry AgNW based textile electrodes. (c) Pictures showing the configuration of EMG measurements. (d) Comparison of EMG signals between commercial gel electrodes and dry AgNW based textile electrodes.

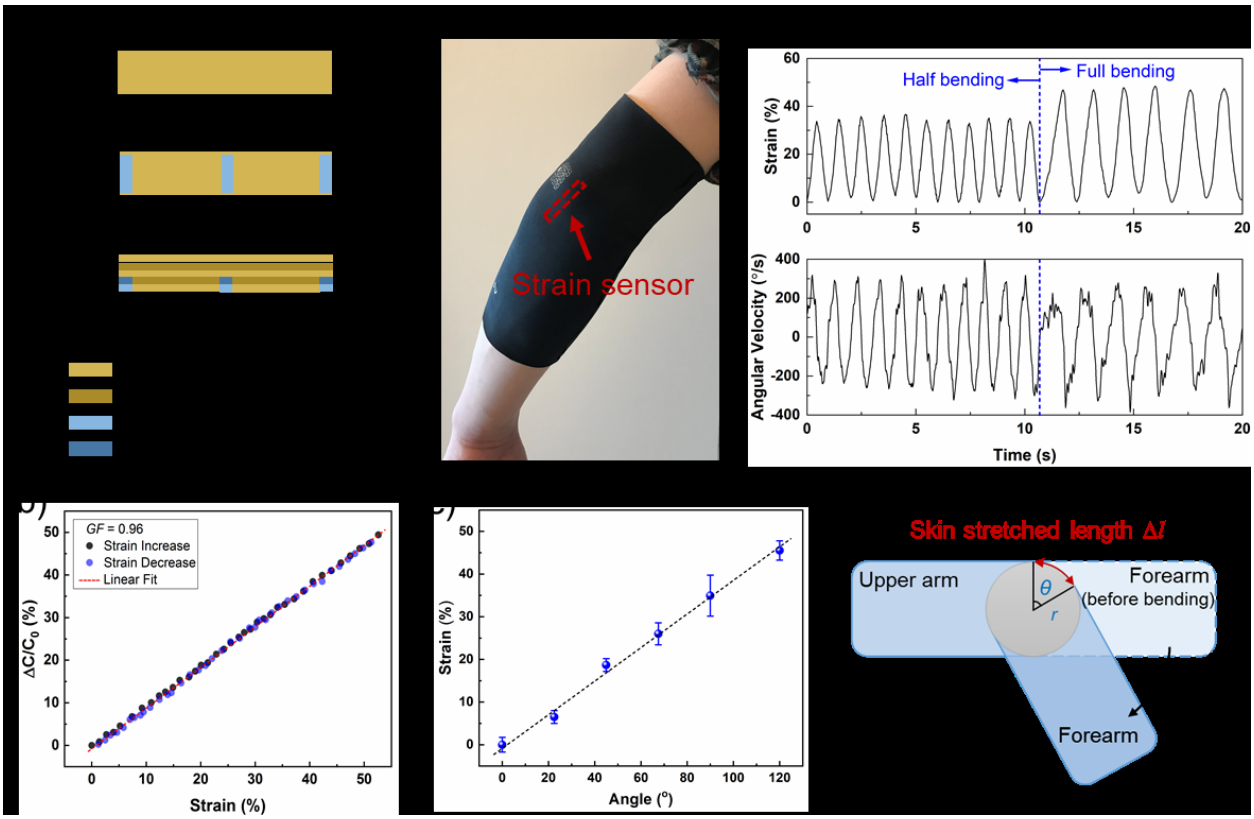

Figure 5. Performance of textile integrated capacitive strain sensors for motion tracking. (a) Schematics showing the structure of the textile integrated capacitive strain sensor. (b) Calibration curve for the textile integrated capacitive strain sensor during strain increase and decrease. (c) A picture showing the placement of the textile patch for elbow bending tracking. (d) Strain and acceleration as a function of time during fast and slow elbow bending. (e) The strain associated with different elbow bending angle. (f) Simplified model for elbow bending.

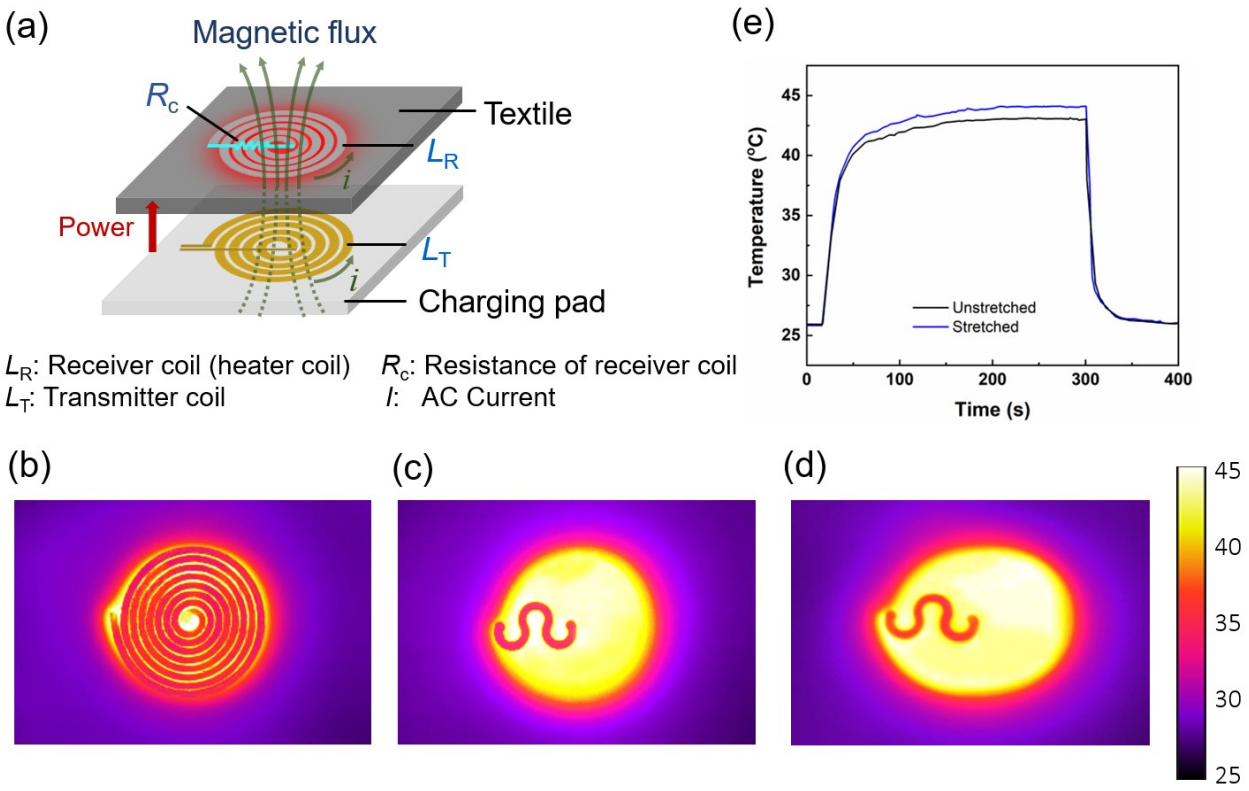

Figure 6. Performance of textile integrated wireless heater. (a) Schematic illustration of the mechanism for wireless heating. IR images showing the temperature distribution of (b) the front of the heater, (c) the backside of the heater, and (d) the backside of the stretched (30%) heater. (e) Time-dependent temperature profiles for the unstretched and stretched heater.

ASSOCIATED CONTENT

Supporting Information

SEM image of AgNWs coated on glass substrate before encapsulation with TPU; Cross-sectional SEM image of the AgNW/TPU composite; Schematics of the laser scribing process; SEM images of the laser scribing line of AgNW/TPU composite and AgNW networks; Resistance change of AgNW/TPU patterns laminated on pretrained textiles as a function of strain; Relative changes in resistance of AgNW/TPU patterns laminated on textiles during 1000 cycles of scrubbing against skin surface; Water vapor transmission of original and AgNW/TPU laminated E-textiles; Photograph showing the skin surface after attaching the E-textile for 1 week; Electrode-skin impedance; ECG measurements and EMG measurements for commercial gel electrodes, dry AgNW based textile electrodes, stretched AgNW based textile electrodes, and washed AgNW based textile electrodes, respectively; Stability test of the fabricated capacitive strain sensor. The Supporting Information is available free of charge on the ACS Publications website.

AUTHOR INFORMATION

Corresponding Author

*E-mail: yong_zhu@ncsu.edu

ACKNOWLEDGMENTS

The authors gratefully acknowledge the financial support from the National Science Foundation (NSF) through Award Nos. IIS-1637892 and CMMI-1728370.

REFERENCES

1. Rogers, J. A.; Someya, T.; Huang, Y. Materials and Mechanics for Stretchable Electronics. *Science* **2010**, *327*, 1603-1607.
2. Trung, T. Q.; Lee, N. E. Flexible and Stretchable Physical Sensor Integrated Platforms for Wearable Human-Activity Monitoring and Personal Healthcare. *Adv. Mater.* **2016**, *28*, 4338-4372.
3. Khan, Y.; Ostfeld, A. E.; Lochner, C. M.; Pierre, A.; Arias, A. C. Monitoring of Vital Signs with Flexible and Wearable Medical Devices. *Adv. Mater.* **2016**, *28*, 4373-4395.
4. Yao, S.; Swetha, P.; Zhu, Y. Nanomaterial-Enabled Wearable Sensors for Healthcare. *Adv. Healthc. Mater.* **2018**, *7*, 1700889.
5. Wang, T.; Yang, H.; Qi, D.; Liu, Z.; Cai, P.; Zhang, H.; Chen, X. Mechano-Based Transductive Sensing for Wearable Healthcare. *Small* **2018**, *14*, 1702933.
6. Gao, W.; Emaminejad, S.; Nyein, H. Y. Y.; Challa, S.; Chen, K.; Peck, A.; Fahad, H. M.; Ota, H.; Shiraki, H.; Kiriya, D.; Lien, D.-H.; Brooks, G. A.; Davis, R. W.; Javey, A. Fully Integrated Wearable Sensor Arrays for Multiplexed in Situ Perspiration Analysis. *Nature* **2016**, *529*, 509-514.
7. Huang, Z.; Hao, Y.; Li, Y.; Hu, H.; Wang, C.; Nomoto, A.; Pan, T.; Gu, Y.; Chen, Y.; Zhang, T.; Li, W.; Lei, Y.; Kim, N.; Wang, C.; Zhang, L.; Ward, J. W.; Maralani, A.; Li, X.; Durstock, M. F.; Pisano, A.; Lin, Y.; Xu, S. Three-Dimensional Integrated Stretchable Electronics. *Nat. Electron.* **2018**, *1*, 473-480.
8. Son, D.; Kang, J.; Vardoulis, O.; Kim, Y.; Matsuhisa, N.; Oh, J. Y.; To, J. W.; Mun, J.; Katsumata, T.; Liu, Y.; McGuire, A. F.; Krason, M.; Molina-Lopez, F.; Ham, J.; Kraft, U.; Lee, Y.; Yun, Y.; Tok, J. B.-H.; Bao, Z. An Integrated Self-Healable Electronic Skin System Fabricated Via Dynamic Reconstruction of a Nanostructured Conducting Network. *Nat. Nanotechnol.* **2018**, *13*, 1057-1065.
9. Kim, H.-J.; Sim, K.; Thukral, A.; Yu, C. Rubbery Electronics and Sensors from Intrinsically Stretchable Elastomeric Composites of Semiconductors and Conductors. *Sci. Adv.* **2017**, *3*, e1701114.
10. Lim, S.; Son, D.; Kim, J.; Lee, Y. B.; Song, J. K.; Choi, S.; Lee, D. J.; Kim, J. H.; Lee, M.; Hyeon, T.; Kim, D.-H. Transparent and Stretchable Interactive Human Machine Interface Based on Patterned Graphene Heterostructures. *Adv. Funct. Mater.* **2015**, *25*, 375-383.
11. Wang, X.; Zhang, Y.; Zhang, X.; Huo, Z.; Li, X.; Que, M.; Peng, Z.; Wang, H.; Pan, C. A Highly Stretchable Transparent Self-Powered Triboelectric Tactile Sensor with Metallized Nanofibers for Wearable Electronics. *Adv. Mater.* **2018**, *30*, 1706738.
12. Lee, H.; Choi, T. K.; Lee, Y. B.; Cho, H. R.; Ghaffari, R.; Wang, L.; Choi, H. J.; Chung, T. D.; Lu, N.; Hyeon, T.; Choi, S. H.; Kim, D.-H. A Graphene-Based Electrochemical Device with Thermoresponsive Microneedles for Diabetes Monitoring and Therapy. *Nat. Nanotechnol.* **2016**, *11*, 566-572.
13. Kim, D.-H.; Lu, N.; Ma, R.; Kim, Y.-S.; Kim, R.-H.; Wang, S.; Wu, J.; Won, S. M.; Tao, H.; Islam, A.; Yu, K. J.; Kim, T.-i.; Chowdhury, R.; Ying, M.; Xu, L.; Li, M.; Chung, H.-J.; Keum, H.; McCormick, M.; Liu, P.; Zhang, Y.-W.; Omenetto, F. G.; Huang, Y.; Coleman, T.; Rogers, J. A. Epidermal Electronics. *Science* **2011**, *333*, 838-843.
14. Sun, B.; McCay, R. N.; Goswami, S.; Xu, Y.; Zhang, C.; Ling, Y.; Lin, J.; Yan, Z. Gas-Permeable, Multifunctional on-Skin Electronics Based on Laser-Induced Porous Graphene and Sugar-Templated Elastomer Sponges. *Adv. Mater.* **2018**, *30*, 1804327.

15. Miyamoto, A.; Lee, S.; Cooray, N. F.; Lee, S.; Mori, M.; Matsuhisa, N.; Jin, H.; Yoda, L.; Yokota, T.; Itoh, A. Inflammation-Free, Gas-Permeable, Lightweight, Stretchable on-Skin Electronics with Nanomeshes. *Nat. Nanotechnol.* **2017**, *12*, 907-913.
16. Castano, L. M.; Flatau, A. B. Smart Fabric Sensors and E-Textile Technologies: A Review. *Smart Mater. Struct.* **2014**, *23*, 053001.
17. Heo, J. S.; Eom, J.; Kim, Y. H.; Park, S. K. Recent Progress of Textile-Based Wearable Electronics: A Comprehensive Review of Materials, Devices, and Applications. *Small* **2018**, *14*, 1703034.
18. Zeng, W.; Shu, L.; Li, Q.; Chen, S.; Wang, F.; Tao, X. M. Fiber-Based Wearable Electronics: A Review of Materials, Fabrication, Devices, and Applications. *Adv. Mater.* **2014**, *26*, 5310-5336.
19. Pang, S.; Gao, Y.; Choi, S. Flexible and Stretchable Biobatteries: Monolithic Integration of Membrane-Free Microbial Fuel Cells in a Single Textile Layer. *Adv. Energy Mater.* **2018**, *8*, 1702261.
20. Liao, X.; Song, W.; Zhang, X.; Huang, H.; Wang, Y.; Zheng, Y. Directly Printed Wearable Electronic Sensing Textiles Towards Human-Machine Interfaces. *J. Mater. Chem. C* **2018**, *6*, 12841-12848.
21. Liao, X.; Wang, W.; Wang, L.; Tang, K.; Zheng, Y. Controllably Enhancing Stretchability of Highly Sensitive Fiber-Based Strain Sensors for Intelligent Monitoring. *ACS Appl. Mater. Interfaces* **2018**, *11*, 2431-2440.
22. Cao, R.; Pu, X.; Du, X.; Yang, W.; Wang, J.; Guo, H.; Zhao, S.; Yuan, Z.; Zhang, C.; Li, C.; Wang, Z. L. Screen-Printed Washable Electronic Textiles as Self-Powered Touch/Gesture Tribo-Sensor for Intelligent Human-Machine Interaction. *ACS Nano* **2018**, *12*, 5190-5196.
23. Yin, Z.; Jian, M.; Wang, C.; Xia, K.; Liu, Z.; Wang, Q.; Zhang, M.; Wang, H.; Liang, X.; Liang, X. Splash-Resistant and Light-Weight Silk-Sheathed Wires for Textile Electronics. *Nano Lett.* **2018**, *18*, 7085-7091.
24. Yokus, M. A.; Foote, R.; Jur, J. S. Printed Stretchable Interconnects for Smart Garments: Design, Fabrication, and Characterization. *IEEE Sens. J.* **2016**, *16*, 7967-7976.
25. Jin, H.; Matsuhisa, N.; Lee, S.; Abbas, M.; Yokota, T.; Someya, T. Enhancing the Performance of Stretchable Conductors for E-Textiles by Controlled Ink Permeation. *Adv. Mater.* **2017**, *29*, 1605848.
26. Wills, K.; Krzyzak, K.; Bush, J.; Ashayer-Soltani, R.; Graves, J.; Hunt, C.; Cobley, A. Additive Process for Patterned Metallized Conductive Tracks on Cotton with Applications in Smart Textiles. *J. Text. I.* **2018**, *109*, 268-277.
27. Suikkola, J.; Björninen, T.; Mosallaei, M.; Kankkunen, T.; Iso-Ketola, P.; Ukkonen, L.; Vanhala, J.; Mäntysalo, M. Screen-Printing Fabrication and Characterization of Stretchable Electronics. *Sci. Rep.* **2016**, *6*, 25784.
28. Vervust, T.; Buyle, G.; Bossuyt, F.; Vanfleteren, J. Integration of Stretchable and Washable Electronic Modules for Smart Textile Applications. *J. Text. I.* **2012**, *103*, 1127-1138.
29. Jang, K.-I.; Han, S. Y.; Xu, S.; Mathewson, K. E.; Zhang, Y.; Jeong, J.-W.; Kim, G.-T.; Webb, R. C.; Lee, J. W.; Dawidczyk, T.; Kim, R. H.; Song, Y. M.; Yeo, W.-H.; Kim, S.; Cheng, H.; Rhee, S. I.; Chung, J.; Kim, B.; Chung, H. U.; Lee, D.; Yang, Y.; Cho, M.; Gaspar, J. G.; Carbonari, R.; Fabiani, M.; Gratton, G.; Huang, Y.; Rogers, J. A. Rugged and Breathable Forms of Stretchable Electronics with Adherent Composite Substrates for Transcutaneous Monitoring. *Nat. Commun.* **2014**, *5*, 4779.
30. Yao, S.; Zhu, Y. Nanomaterial-Enabled Stretchable Conductors: Strategies, Materials and Devices. *Adv. Mater.* **2015**, *27*, 1480-1511.

31. Tokuno, T.; Nogi, M.; Karakawa, M.; Jiu, J.; Nge, T. T.; Aso, Y.; Suganuma, K. Fabrication of Silver Nanowire Transparent Electrodes at Room Temperature. *Nano Res.* **2011**, *4*, 1215-1222.
32. Langley, D.; Lagrange, M.; Giusti, G.; Jimenez, C.; Bréchet, Y.; Nguyen, N. D.; Bellet, D. Metallic Nanowire Networks: Effects of Thermal Annealing on Electrical Resistance. *Nanoscale* **2014**, *6*, 13535-13543.
33. Xu, F.; Zhu, Y. Highly Conductive and Stretchable Silver Nanowire Conductors. *Advanced Materials* **2012**, *24*, 5117-5122.
34. Fan, J. A.; Yeo, W.-H.; Su, Y.; Hattori, Y.; Lee, W.; Jung, S.-Y.; Zhang, Y.; Liu, Z.; Cheng, H.; Falgout, L.; Bajema, M.; Coleman, T.; Gregoire, D.; Larsen, R. J.; Huang, Y.; Rogers, J. A. Fractal Design Concepts for Stretchable Electronics. *Nat. Commun.* **2014**, *5*, 3266.
35. Tao, X.; Huang, T. H.; Shen, C. L.; Ko, Y. C.; Jou, G. T.; Koncar, V. Bluetooth Low Energy-Based Washable Wearable Activity Motion and Electrocardiogram Textronic Monitoring and Communicating System. *Adv. Mater. Technol.* **2018**, *3*, 1700309.
36. Yu, L.; Yeo, J. C.; Soon, R. H.; Yeo, T.; Lee, H. H.; Lim, C. T. Highly Stretchable, Weavable, and Washable Piezoresistive Microfiber Sensors. *ACS Appl. Mater. Interfaces* **2018**, *10*, 12773-12780.
37. Zhao, Z.; Yan, C.; Liu, Z.; Fu, X.; Peng, L. M.; Hu, Y.; Zheng, Z. Machine-Washable Textile Triboelectric Nanogenerators for Effective Human Respiratory Monitoring through Loom Weaving of Metallic Yarns. *Adv. Mater.* **2016**, *28*, 10267-10274.
38. Tao, X.; Koncar, V.; Huang, T.-H.; Shen, C.-L.; Ko, Y.-C.; Jou, G.-T. How to Make Reliable, Washable, and Wearable Textronic Devices. *Sensors* **2017**, *17*, 673.
39. Ankhili, A.; Tao, X.; Cochrane, C.; Coulon, D.; Koncar, V. Washable and Reliable Textile Electrodes Embedded into Underwear Fabric for Electrocardiography (ECG) Monitoring. *Materials* **2018**, *11*, 256.
40. Jiang, S.; Teng, C. P. Fabrication of Silver Nanowires-Loaded Polydimethylsiloxane Film with Antimicrobial Activities and Cell Compatibility. *Mater. Sci. Eng. C* **2017**, *70*, 1011-1017.
41. Yao, S.; Zhu, Y. Nanomaterial-Enabled Dry Electrodes for Electrophysiological Sensing: A Review. *JOM* **2016**, *68*, 1145-1155.
42. Yao, S.; Zhu, Y. Wearable Multifunctional Sensors Using Printed Stretchable Conductors Made of Silver Nanowires. *Nanoscale* **2014**, *6*, 2345-2352.
43. Yao, S.; Vargas, L.; Zhu, Y.; Hu, X. A Novel Finger Kinematic Tracking Method Based on Skin-Like Wearable Strain Sensors. *IEEE Sens. J.* **2017**, *18*, 3010-3015.
44. Amjadi, M.; Kyung, K. U.; Park, I.; Sitti, M. Stretchable, Skin-Mountable, and Wearable Strain Sensors and Their Potential Applications: A Review. *Adv. Funct. Mater.* **2016**, *26*, 1678-1698.
45. Park, J. J.; Hyun, W. J.; Mun, S. C.; Park, Y. T.; Park, O. O. Highly Stretchable and Wearable Graphene Strain Sensors with Controllable Sensitivity for Human Motion Monitoring. *ACS Appl. Mater. Interfaces* **2015**, *7*, 6317-6324.
46. Wessendorf, A. M.; Newman, D. J. Dynamic Understanding of Human-Skin Movement and Strain-Field Analysis. *IEEE Trans. Biomed. Eng.* **2012**, *59*, 3432-3438.
47. Cohen, D. J.; Mitra, D.; Peterson, K.; Maharbiz, M. M. A Highly Elastic, Capacitive Strain Gauge Based on Percolating Nanotube Networks. *Nano Lett.* **2012**, *12*, 1821-1825.
48. Nakamoto, H.; Ootaka, H.; Tada, M.; Hirata, I.; Kobayashi, F.; Kojima, F. Stretchable Strain Sensor with Anisotropy and Application for Joint Angle Measurement. *IEEE Sens. J.* **2016**, *16*, 3572-3579.

49. Dehghan, M.; FarahbOD, F. The Efficacy of Thermotherapy and Cryotherapy on Pain Relief in Patients with Acute Low Back Pain, a Clinical Trial Study. *J. Clin. Diagn. Res.* **2014**, *8*, LC01.
50. Malanga, G. A.; Yan, N.; Stark, J. Mechanisms and Efficacy of Heat and Cold Therapies for Musculoskeletal Injury. *Postgrad. Med.* **2015**, *127*, 57-65.
51. Rahimi, R.; Shams Es-haghi, S.; Chittiboyina, S.; Mutlu, Z.; Lelièvre, S. A.; Cakmak, M.; Ziaie, B. Laser-Enabled Processing of Stretchable Electronics on a Hydrolytically Degradable Hydrogel. *Adv. Healthc. Mater.* **2018**, *7*, 1800231.
52. Han, S.; Kim, M. K.; Wang, B.; Wie, D. S.; Wang, S.; Lee, C. H. Mechanically Reinforced Skin-Electronics with Networked Nanocomposite Elastomer. *Adv. Mater.* **2016**, *28*, 10257-10265.
53. Okada, K.; Yamaguchi, T.; Minowa, K.; Inoue, N. The Influence of Hot Pack Therapy on the Blood Flow in Masseter Muscles. *J. Oral. Rehabil.* **2005**, *32*, 480-486.
54. Yao, S.; Cui, J.; Cui, Z.; Zhu, Y. Soft Electrothermal Actuators Using Silver Nanowire Heaters. *Nanoscale* **2017**, *9*, 3797-3805.
55. Hsu, P.-C.; Liu, X.; Liu, C.; Xie, X.; Lee, H. R.; Welch, A. J.; Zhao, T.; Cui, Y. Personal Thermal Management by Metallic Nanowire-Coated Textile. *Nano Lett.* **2014**, *15*, 365-371.
56. Chee, P. S.; Minjal, M. N.; Leow, P. L.; Ali, M. S. M. Wireless Powered Thermo-Pneumatic Micropump Using Frequency-Controlled Heater. *Sens. Actuators. A Phys.* **2015**, *233*, 1-8.
57. Huang, Q.; Zhu, Y. Gravure Printing of Water-Based Silver Nanowire Ink on Plastic Substrate for Flexible Electronics. *Sci. Rep.* **2017**, *8*, 15167.
58. Liang, J.; Tong, K.; Pei, Q. A Water-Based Silver-Nanowire Screen-Print Ink for the Fabrication of Stretchable Conductors and Wearable Thin-Film Transistors. *Adv. Mater.* **2016**, *28*, 5986-5996.
59. Cui, Z.; Han, Y.; Huang, Q.; Dong, J.; Zhu, Y. Electrohydrodynamic Printing of Silver Nanowires for Flexible and Stretchable Electronics. *Nanoscale* **2018**, *10*, 6806-6811.
60. Lee, H.; Seong, B.; Kim, J.; Jang, Y.; Byun, D. Direct Alignment and Patterning of Silver Nanowires by Electrohydrodynamic Jet Printing. *Small* **2014**, *10*, 3918-3922.
61. Huang, Q.; Al-Milaji, K. N.; Zhao, H. Inkjet Printing of Silver Nanowires for Stretchable Heaters. *ACS Appl. Nano Mater.* **2018**, *1*, 4528-4536.
62. Cui, Z.; Poblete, F. R.; Cheng, G.; Yao, S.; Jiang, X.; Zhu, Y. Design and Operation of Silver Nanowire Based Flexible and Stretchable Touch Sensors. *J. Mater. Res.* **2015**, *30*, 79-85.
63. Yao, S.; Myers, A.; Malhotra, A.; Lin, F.; Bozkurt, A.; Muth, J. F.; Zhu, Y. A Wearable Hydration Sensor with Conformal Nanowire Electrodes. *Adv. Healthc. Mater.* **2017**, *6*, 1601159.
64. Song, L.; Myers, A. C.; Adams, J. J.; Zhu, Y. Stretchable and Reversibly Deformable Radio Frequency Antennas Based on Silver Nanowires. *Appl. Mater. Interfaces* **2014**, *6*, 4248-4253.
65. Smits, F. Measurement of Sheet Resistivities with the Four-Point Probe. *Bell Syst. Tech. J.* **1958**, *37*, 711-718.

For Table of Contents Only